Received 13 April 2021; revised 19 May 2021; accepted 25 May 2021. Date of publication 31 May 2021; date of current version 14 June 2021.
The review of this article was arranged by Editor Z. Zhang.

Digital Object Identifier 10.1109/JEDS.2021.3085135

Highly Sensitive Piezoresistive Sensors Based on a Voltage Divider Circuit With TFTs for Ultra-Low Pressure Detection

JIAYU FENG, LONGLONG CHEN, XIFENG LI, AND JIANHUA ZHANG

Key Laboratory of Advanced Display and System Application, Ministry of Education, Shanghai University, Shanghai 200072, China

CORRESPONDING AUTHOR: X. LI (e-mail: lixifeng@shu.edu.cn)

This work was supported in part by the National Key Research and Development Program of China under Grant 2017YFB0404703; in part by the National Natural Science Foundation of China under Grant 61674101; in part by Shanghai Science and Technology Commission under Grant 17DZ2291500 and Grant 16JC1403700; in part by the Program of Shanghai Academic/Technology Research Leader under Grant 18XD1424400; and in part by "Shogun Program" through Shanghai Education Development Foundation and Shanghai Municipal Education Commission.

ABSTRACT A highly sensitive piezoresistive tactile sensor combined with the thin-film transistors (TFTs) is produced in this letter. The sensor uses two-dimensional Ti_3C_2-MXenes as piezoresistive material which is one type of transition metal carbide, nitride and/or carbonitride with a lamellar structure. A voltage divider circuit is designed by connecting piezoresistive material with TFT technology. TFT works in the subthreshold and saturation region during the sensing process to ensure that the magnitude change of current is measured in a small voltage range. The tactile sensor shows high sensitivity of 4636.1 kPa^{-1}, ultra-low tactile detection of 0.98 Pa, and extremely durability for 1,500 sensing cycles. Resultantly, the sensor demonstrates excellent potential for electronic touchscreens and advanced medical testing.

INDEX TERMS Piezoresistive, TFTs, voltage divider circuit, ultra-low tactile detection.

I. INTRODUCTION

As human beings gradually enter the intelligent society, sensors will be widely used in many fields, such as human-machine interface, on-line medical care, intelligent skin and so on [1]–[3]. The tactile sensor is an extremely important kind of sensor, which can directly collect and analyze the position and value information of the human body. And then they transmit and respond electrical signals accordingly. Currently, the commonly used modes of mechanical information acquisition are piezo-electric [4], piezo-capacitive [5] and piezo-resistive [6]. Among them, piezoresistive has become a research hotspot because of its high response sensitivity, wide response range, low cost and durability [7]–[9].

Recently, a kind of MXenes Ti_3C_2 sensor was studied because it can be used in tactile loading detection [10]. It has been proven that Ti_3C_2 can detect external pressure signals precisely due to its high electrical conductivity and large specific surface area [11]–[13]. The fabrication technology and stable performance of Ti_3C_2 are outstanding among the MXenes. The resistance of sensor is controlled by a variable layer distance under tactile pressure, rather than the insertion and removal of ions [11]. Nevertheless, traditional sensors which use MXenes are slightly complicated for large-scale integration [7] and less sensitive to ultra-low pressure detection [13]. Thin film transistors (TFTs) technology has been successfully used in large-scale integration, such as display panels [14], sensor devices [15] and so on, owing to its advantages of small-size, low-cost and amplification effect. It approves that the gate voltage and the source-drain current are used as the basic sensor signals extracted from the TFTs [16]. In the saturated region of TFT, the slight pressure change can even lead to the obvious magnitude change of current. However, the change of current measured by a separate voltage divider without TFT is not obviously enough to be subdivided [17]. So, it is hard for the device without TFT to detect the pressure which is loaded in a small range. And the sensitivity of the device without TFT is lower than that of devices with TFT. Therefore, it is necessary to explore a new and high-performance tactile sensor connecting TFTs

TABLE 1. V_G and R_{MX} under different pressure.

Pressure (Pa)	Resistance (kΩ)	V_G (V)
0	15	2.1
0.98	10	2.47
1.96	9.2	2.9
9.8	6.5	3.5
29.4	5.2	4.5
49	4.1	4.7
58.8	3.7	5.4
127.4	2.5	6
196	2.1	6.3
294	1.2	7.7

with piezoresistive units. Meanwhile, the stability, the on-off ratio and the amplification of TFT are also crucial to the stability and sensitivity of the sensor. The a-IGZO TFT shows its applicability to tactile sensors due to its excellent characteristics and low manufacturing cost, which has the potential for large-area fabrication [18]–[19].

In this letter, a tactile sensor was manufactured and connected to a voltage divider circuit, TFT, which is compatible with display technology. During the sensing process, TFT worked at the subthreshold and saturation region to ensure that the current signal was amplified, and the magnitude changes of source-drain current were detected with a small shift of gate voltage caused by tactile pressure. The novel design makes the sensor have ultra-low tactile detection limit, high sensitivity and can be used in large-area integration.

II. EXPERIMENTAL

The whole circuit including interdigital electrodes, TFTs and square resistances, is designed and manufactured on a 200 mm × 200 mm glass substrate. The bottom-gate, top source/drain TFT configuration was adopted. A 150-nm-thick molybdenum (Mo) film was grown by sputtering and was patterned as gate electrode. And interdigital electrode of sensors was prepared at the same time. Subsequently, a 300-nm-thick SiN_X and 100-nm-thick SiO_X dielectric film was deposited as gate isolate layer by PECVD. The a-IGZO film with a thickness of 50 nm was grown as the active channel layer at room temperature by sputtering. Then 200 nm SiO_X was grown as etching stopper layer and 100 nm Mo was sputtered as source-drain metal. Finally, 200 nm SiO_X passivation layer was deposited to prevent the damage of water and oxygen in air and 50nm thick ITO was sputtered as resistance of the circuit. Patterns were produced by photolithography. The circuit is annealed at 200 °C for 2 hours. The structure diagram of the device obtained by photolithography is depicted in Fig. 1. Then, the MAX phase precursor (Ti_3C_2) powder was prepared by etching the MAX phase precursor (Ti_3AlC_2) [13], [17]. And the piezoresistive tactile sensor was obtained by dropping Ti_3C_2 solution on the glass and heating at 80 °C for 15 minutes, and inverting the glass encapsulation with Ti_3C_2 on the interdigital electrode.

The static pressure was provided by weights of different masses, and dynamic pressure was loaded by an acquisition

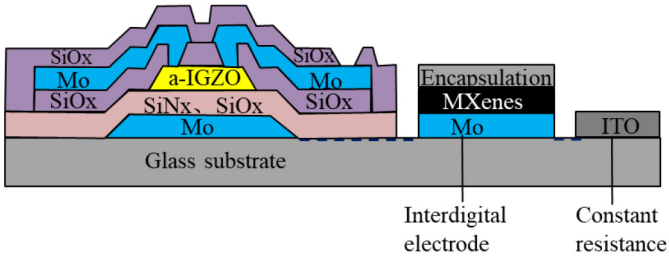

FIGURE 1. The structure diagram of the device.

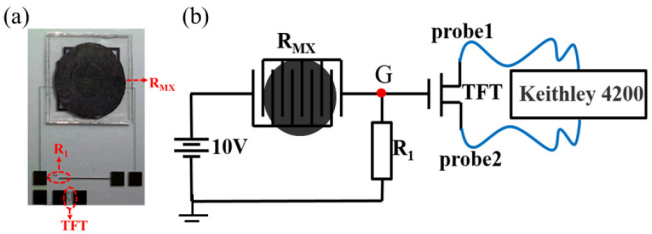

FIGURE 2. (a) Photograph of the fabricated tactile sensor. (b) Circuit diagram of the sensor.

analyzer (DH5922N, D.H.) and a scanning signal generator (DH-1301, D.H.). The characteristic parameters of the tactile sensor were measured by a constant voltage source. A semiconductor parameter analyzer (4200-SCS, Keithley) was used to record transfer characteristics of TFT and the performance of the sensor.

III. RESULTS AND DISCUSSION

The image of the tactile sensor is illustrated in Fig. 2(a). The sensing device comprises three parts as shown in Fig. 2(b): 10V DC input voltage V_{in}, two resistors (variable piezoresistor R_{MX} and constant R_1) for voltage division, and TFT unit. The source and drain electrodes of the TFT are connected to the probes of Keithey 4200. R_{MX} decreased when the tactile pressure was applied on the sensor. The value of MXenes' initial resistance (at 0 Pa) is 15 kΩ and R_1 is 4 kΩ. The gate voltage of TFT V_G, which changes with the change of R_{MX} according to the circuit diagram, can be described as following:

$$V_G = V_{in} * \frac{R_1}{R_1 + R_{MX}} \tag{1}$$

During the sensing process, TFT works in the subthreshold and saturation region to ensure that response current signals can be measured and amplified by orders of magnitude with a slight change in piezoresistor. Therefore the sensitivity of the tactile sensor is greatly improved.

In addition, the transfer characteristic curve of TFT device is as depicted in Fig. 3. It could be indicated that the threshold voltage of the TFT device is 0.2 V and on-off ratio is 10^6. The changes of R_{MX} can be amplified into a current signal by TFT The current signal is the drain current of the TFT, which is detected by Keithley 4200. The drain current varies with applied gate voltage by more than three orders

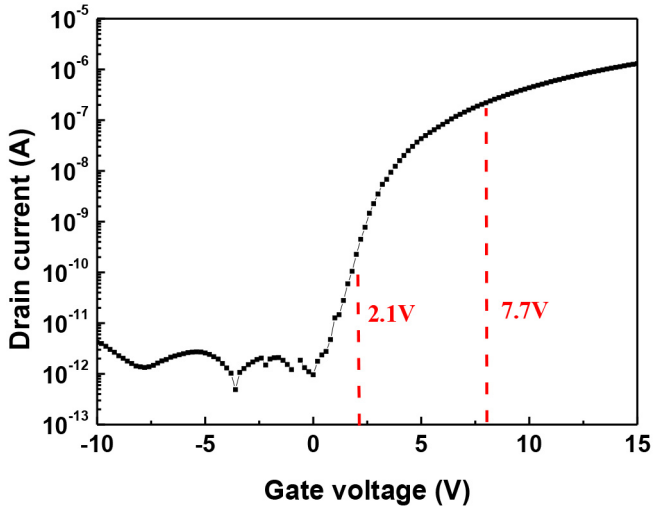

FIGURE 3. Transfer characteristic curve of TFT.

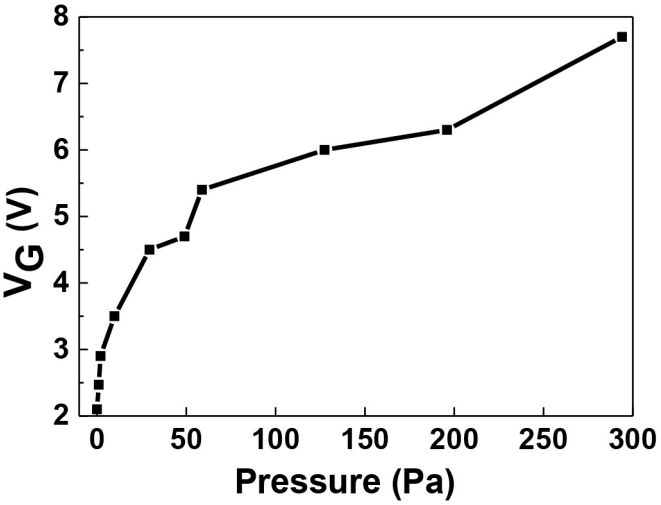

FIGURE 5. V_G under different pressure.

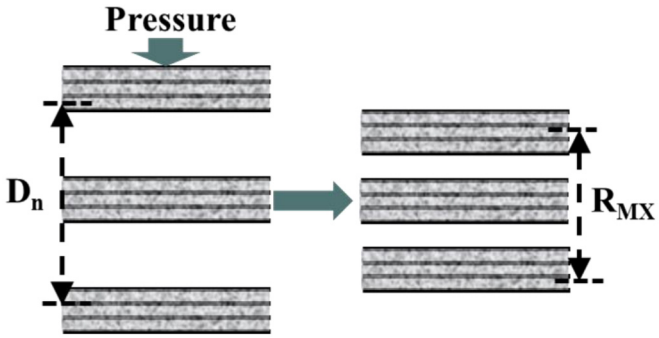

FIGURE 4. Working mechanism diagram of MXenes.

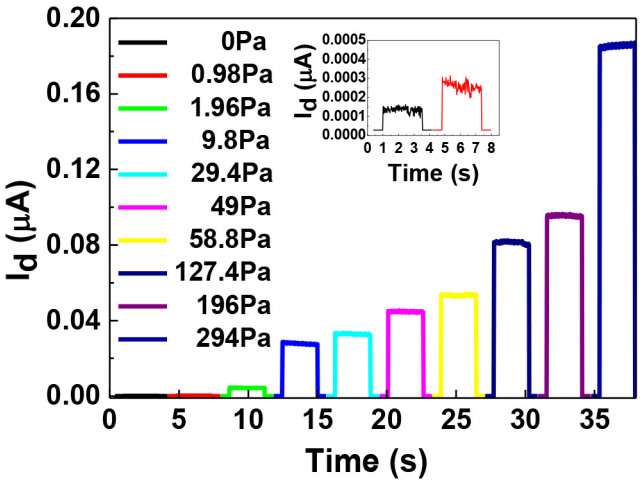

FIGURE 6. Responsive drain current curves under the pressures ranging from 0 Pa to 294 Pa. (Insert: The responsive drain current under 0Pa to 0.98 Pa).

of magnitude when TFT works in the subthreshold and saturation range of 2.1V to 7.7V under a constant drain voltage at 10V, which means the weak touch force can be detected sensitively.

MXenes is a kind of material with variable layer spacing. the layer distance D_n decreases after loading pressure, resulting in the decrease of resistance R_{MX}. Fig. 4 shows the working mechanism diagram of MXenes.

In this paper, the current of the sensor is measured under different pressure from 0 Pa to 294 pa. Table 1 shows the resistance values of MXenes under different pressures and the corresponding gate voltage V_G. Figure 5 shows V_G under different pressures vividly.

Responsive drain current curves with respect to the pressure from 0 Pa to 294 Pa are illustrated in Fig. 6. The drain current of TFT I_d increases monotonically in the subthreshold and saturation region as the pressure increases, which corresponds to the increase in the gate voltage of the TFT from 2.1 V to 7.7 V in the subthreshold and saturation region. At the same time, the voltage across the R_{MX} is decreasing. It indicates that the resistance of the sensing unit decreases with the increase of pressure. The working micromechanism of the sensing unit can explain its conductive performance. The total resistance of the sensing unit is defined as $R_{MX} = R_{MX}' + R_{con}$, where R_{MX}' is the resistance of Ti_3C_2-MXenes itself, and R_{con} is the contact resistance between the interdigital electrodes and Ti_3C_2-MXenes. The internal structure of Ti_3C_2-MXenes is unique because the distance between interlayers of Ti_3C_2-MXenes is variable under different pressure. When the applied external pressure increases from 0 Pa to 294 Pa, the distance between neighboring interlayers in Ti_3C_2-MXenes shortens and the conductivity increases which results in the decrease of R_{MX}'. Simultaneously, the tighter contact between the electrodes and Ti_3C_2-MXenes makes the conductive path increase, and then R_{con} decreases. Consequently, and the responsive current increases and R_{MX} decreases from 15 kΩ to 1.2 kΩ under the pressures ranging from 0 Pa to 294 Pa. The decrease in R_{MX} causes the voltage divided by R_1 to rise

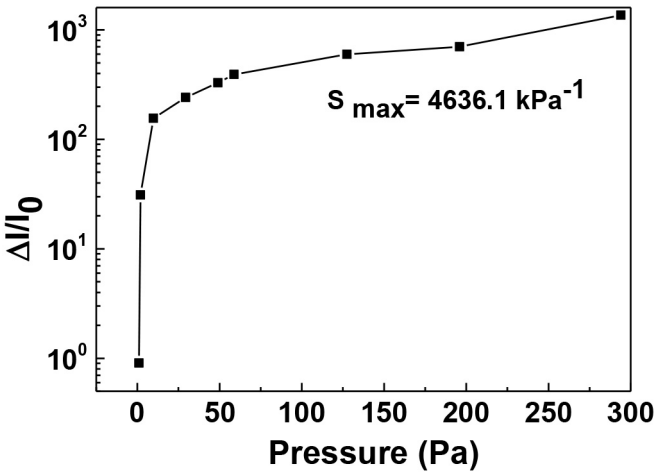

FIGURE 7. Change in current ($\Delta I/I_0$) of the sensor with respect to increased tactile pressures from 0Pa to 294Pa.

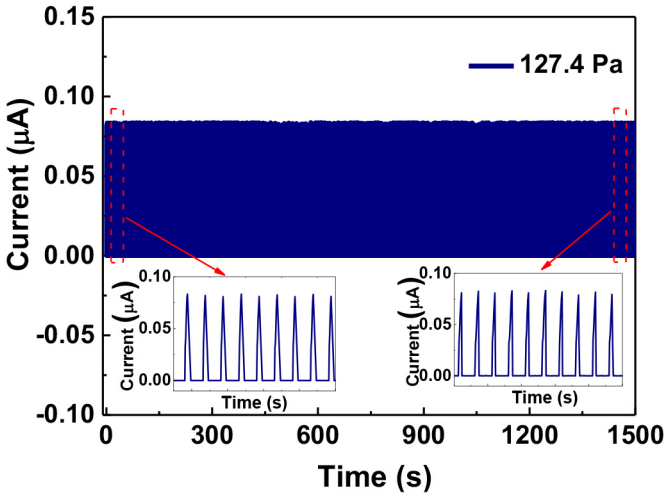

FIGURE 8. Repeatability tests of the sensor for 1500 cycles under 127.4 Pa.

because R_1 is constant resistance in the voltage dividing circuit. Thus, the gate voltage of the TFT increases. Resultantly, the current signal is amplified by TFT in the subthreshold and saturation region from 2.1 V to 7.7 V. It is concluded that the drain current changes by order of magnitude after the tactile pressure loaded from 0 Pa to 294 Pa.

Additionally, the sensitivity of the tactile sensor to pressure is shown in Fig. 7. The sensitivity is defined as $S = (\Delta I/I_0)/\Delta P$, where ΔI is the relative change of I_d, I_0 is the initial I_d under unloading pressure and ΔP is the pressure change. The rate of current change $\Delta I/I_0$ increases from 0 to 1363 as the pressure increases because the distance between electrodes and MXenes shortens and the conductive path increases continuously. The sensitivity curve consistent with the transfer characteristic curve of TFT is non-linear because the current signal originates from the TFT. According to calculations, the sensitivity of the sensor reaches the maximum 4636.1 kPa^{-1} under 294 Pa. It is speculated that the current sensitivity of the sensor is high because I_d is sensitive in the low voltage range when TFT works in the subthreshold and saturation region. The current amplification effect of TFT makes the current signal present three magnitude changes in a small voltage range. Therefore, the piezoresistive sensor has ultra-low pressure detection limit of 0.98 Pa and exhibits high sensitivity in the low tactile range from 0.98 Pa to 294 Pa because of the excellent conductivity of MXenes, the interdigital electrodes and the voltage divider circuit based on TFT.

In order to characterize the repeatability of the piezoresistive sensor with TFT, 1500 cycles of testing (1 s per cycle) are measured by loading/ unloading a pressure of 127.4 Pa. As depicted in Fig. 8, the piezoresistive sensor based on a voltage divider circuit with TFTs can maintain a stable current response even when external tactile signals change rapidly. It can be seen from the figure that the current show no obvious degradation after 1500 pressure cycles. Thus it is proved that the sensor shows good repeatability and high reliability.

IV. CONCLUSION

A high-performance piezoresistive tactile sensor composed of the Ti_3C_2-MXenes and TFTs, with a voltage divider circuit was produced successfully. During the voltage division process, TFT works in the subthreshold and saturation region to ensure that the magnitude change of current is measured in a small voltage range. This novel proposed design makes the sensor highly sensitive (4636.1 kPa^{-1}), highly stable (1500 cycles under 127.4 Pa) and capable of measuring ultra-low pressure (0.98 Pa). These superior characteristics demonstrate the excellent potential of this sensor for electronic touchscreens and advanced medical testing.

REFERENCES

[1] Y. Ding, T. Xu, O. Onyilagha, H. Fong, and Z. Zhu, "Recent advances in flexible and wearable pressure sensors based on piezoresistive 3D monolithic conductive sponges," *ACS Appl. Mater. Interfaces*, vol. 11, pp. 6685–6704, Apr. 2019, doi: 10.1021/acsami.8b20929.

[2] Y. Yang and W. Gao, "Wearable and flexible electronics for continuous molecular monitoring," *Chem. Soc. Rev.*, vol. 48, no. 6, pp. 1465–1491, Apr. 2019, doi: 10.1039/c7cs00730b.

[3] Y. Zang, F. Zhang, C. Di, and D. Zhu, "Advances of flexible pressure sensors toward artificial intelligence and health care applications," *Mater. Horizons*, vol. 2, no. 2, pp. 140–156, Feb. 2015, doi: 10.1039/c4mh00147h.

[4] X. Li and E. C. Kan, "A wireless low-range pressure sensor based on P(VDF-TrFE) piezoelectric resonance," *Sens. Act. A, Phys.*, vol. 163, no. 2, pp. 457–463, Oct. 2010, doi: 10.1016/j.sna.2010.08.022.

[5] C. Xin *et al.*, "Highly sensitive flexible pressure sensor by the integration of microstructured PDMS film with a-IGZO TFTs," *IEEE Electron Device Lett.*, vol. 39, no. 7, pp. 13073–13076, Jul. 2018, doi: 10.1109/LED.2018.2839595.

[6] W. Liu *et al.*, "A flexible and highly sensitive pressure sensor based on elastic carbon foam," *J. Mater. Chem. C.*, vol. 6, pp. 1451–1458, Jun. 2018, doi: 10.1039/C7TC05228F.

[7] Z. Ma *et al.*, "Lightweight, compressible and electrically conductive polyurethane sponges coated with synergistic multiwalled carbon nanotubes and graphene for piezoresistive sensors," *Nanoscale*, vol. 10, pp. 7116–7126, Oct. 2018, doi: 10.1039/C8NR00004B.

[8] D. Niu *et al.*, "Graphene-elastomer nanocomposites based flexible piezoresistive sensors for strain and pressure detection," *Mater. Res. Bull.*, vol. 102, pp. 92–99, Jun. 2018, doi: 10.1016/j.materresbull.2018.02.005.

[9] H. Liu *et al.*, "Lightweight conductive graphene/thermoplastic polyurethane foams with ultrahigh compressibility for piezoresistive sensing," *J. Mater. Chem. C.*, vol. 5, no. 1, pp. 73–83, May 2017, doi: 10.1039/c6tc03713e.

[10] M. Naguib *et al.*, "Two-dimensional nanocrystals produced by exfoliation of Ti_3AlC_2," *Adv. Mater.*, vol. 23, no. 37, pp. 4248–4253, Aug. 2011, doi: 10.1002/adma.201102306.

[11] Y. Ma *et al.*, "A highly flexible and sensitive piezoresistive sensor based on MXene with greatly changed interlayer distances," *Nat. Commun.*, vol. 8, no. 1207, pp. 140–156, Oct. 2017, doi: 10.1038/s41467-017-01136-9.

[12] Y. Ma *et al.*, "3D synergistical mxene/reduced graphene oxide aerogel for a piezoresistive sensor," *ACS Nano*, vol. 12, pp. 3209–3216, Dec. 2018, doi: 10.1021/acsami.7b16975.

[13] T. Li *et al.*, "A flexible pressure sensor based on an MXene–textile network structure," *J. Mater. Chem. C*, vol. 7, pp. 1022–1027, Jul. 2017, doi: 10.1039/c8tc04893b.

[14] W. Huang *et al.*, "Flexible and lightweight pressure sensor based on carbon nanotube/thermoplastic polyurethane-aligned conductive foam with superior compressibility and stability," *ACS Appl. Mater. Interfaces*, vol. 9, pp. 42266–42277, Nov. 2017, doi: 10.1021/acsami.7b16975.

[15] Y.-H. Wu *et al.*, "Channel crack-designed gold@PU sponge for highly elastic piezoresistive sensor with excellent detectability," *ACS Appl. Mater. Interfaces*, vol. 9, pp. 20098–20105, Sep. 2017, doi: 10.1021/acsami.7b04605.

[16] H. Castro, V. Correia, N. Pereira, P. Costab, J. Oliveiraa, and S. Lanceros-Méndez, "Printed Wheatstone bridge with embedded polymer based piezoresistive sensors for strain sensing applications," *Addit. Manuf.*, vol. 20, pp. 119–125, Mar. 2018, doi: 10.1016/j.addma.2018.01.004.

[17] L. Chen, J. Feng, T. Li, X. Li, and J. Zhang, "High-tactile sensitivity of piezoresistive sensors with a micro-crack structure induced by thin film tension," *IEEE Electron Device Lett.*, vol. 40, no. 9, pp. 1519–1521, Sep. 2019, doi: 10.1109/LED.2019.2927720.

[18] K. Nomura, A. Takagi, T. Kamiya, H. Ohta, M. Hirano, and H. Hosono, "Amorphous oxide semiconductors for high-performance flexible thin-film transistors," *Jpn. J. Appl. Phys.*,, vol. 45, no. 5S, pp. 4303–4308, 2006, doi: 10.1143/JJAP.45.4303.

[19] J. K. Jeong, J. H. Jeong, H. W. Yang, J.-S. Park, Y.-G. Mo, and H. D. Kim, "High performance thin film transistors with cosputtered amorphous indium gallium zinc oxide channel," *Appl. Phys. Lett.*, vol. 91, no. 11, 2007, Art. no. 113505, doi: 10.1063/1.2783961.